

Supporting Information

Transparent and Flexible Surface Enhanced Raman Scattering (SERS) Sensors Based on Gold Nanostar Arrays Embedded in Silicon Rubber Film

Seungyoung Park[†], Jiwon Lee[†], Hyunhyub Ko^{†,}*

[†] School of Energy and Chemical Engineering, Ulsan National Institute of Science and Technology (UNIST), Ulsan Metropolitan City, 689-798, Republic of Korea.

* To whom correspondence should be addressed: hyunhko@unist.ac.kr

S1. SERS enhancement factor calculations

For the calculation of SERS enhancement factor (EF) for analyte molecule, we used the following standard equation

$$\text{SERS EF} = \frac{I_{\text{SERS}}/N_{\text{SERS}}}{I_{\text{Ref}}/N_{\text{Ref}}}$$

Where I_{SERS} and I_{Ref} are represented as the characteristic Raman intensity of analyte molecule measured with the SERS substrate and reference substrate, N_{SERS} and N_{Ref} are represented as the number of analyte molecules attended for the SERS and reference substrate. We used the characteristic peaks at 1079 cm^{-1} by C-C stretching mode of the benzenethiol molecules for I_{SERS} and I_{Ref} .

Taking the adsorbate benzenethiol as an example, the largest value of the packing density reported in the literature ($6.8 * 10^{14} \text{ molecules/cm}^2$)

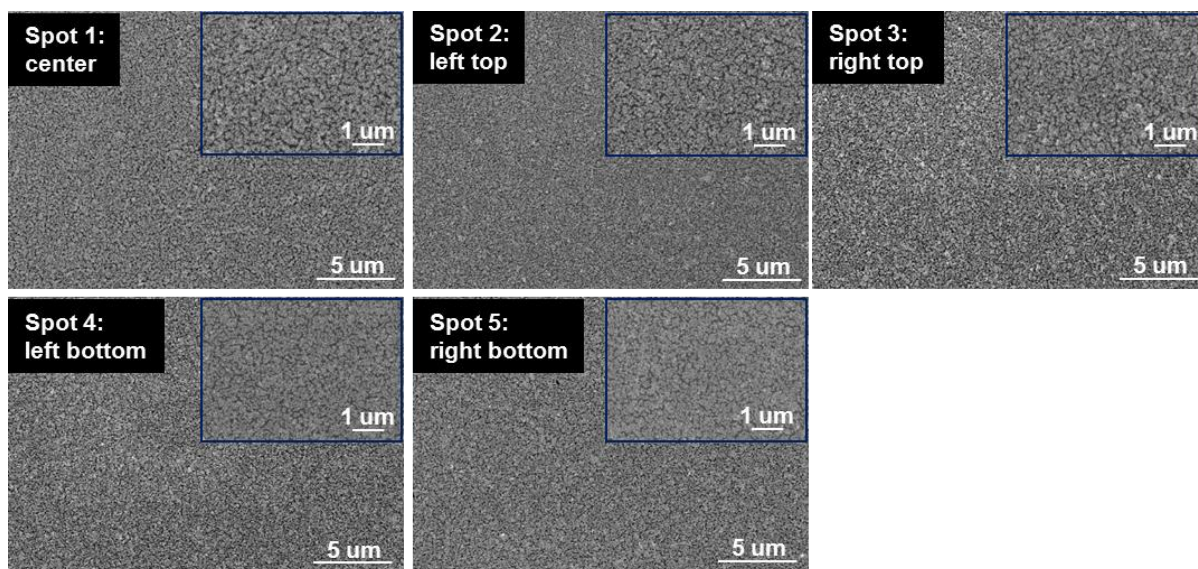


Figure S1 | SEM images of the GNS array on the silicon substrate observed in the different spots (center, left top, right top, left bottom, and right bottom of the silicon substrate which has the GNS array).

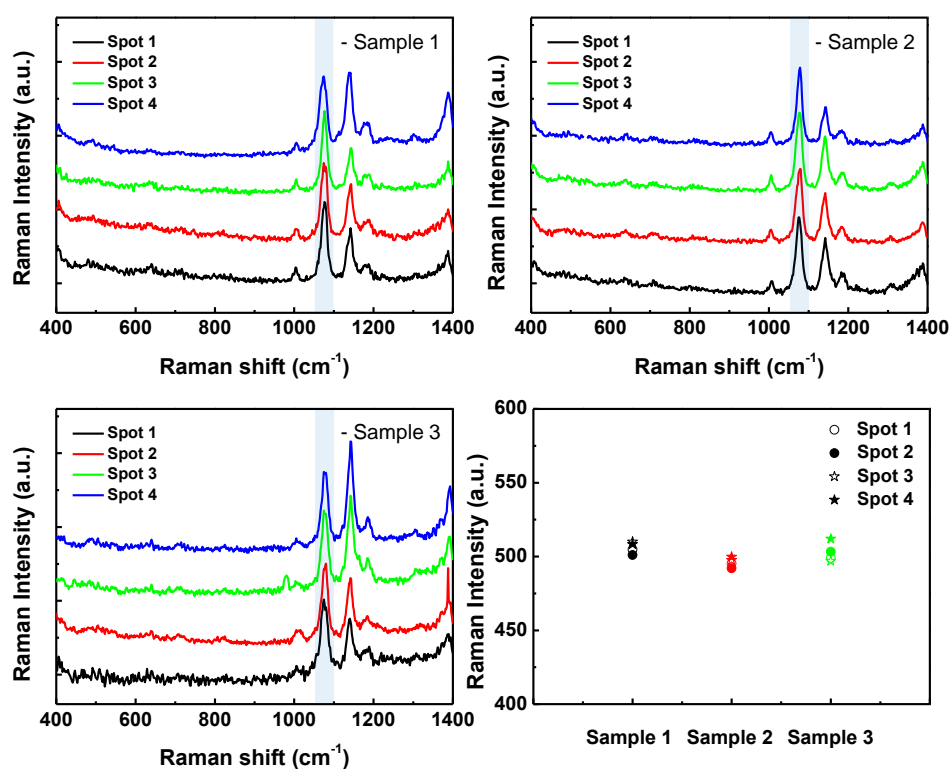


Figure S2 | Raman spectra observed in the different spots (4 spots) with the different samples (3 samples) and the summarized SERS intensity (the comparison with the Raman fingerprint peak at 1071 cm^{-1}) to demonstrate the uniformity and reproducibility of SERS sensor.

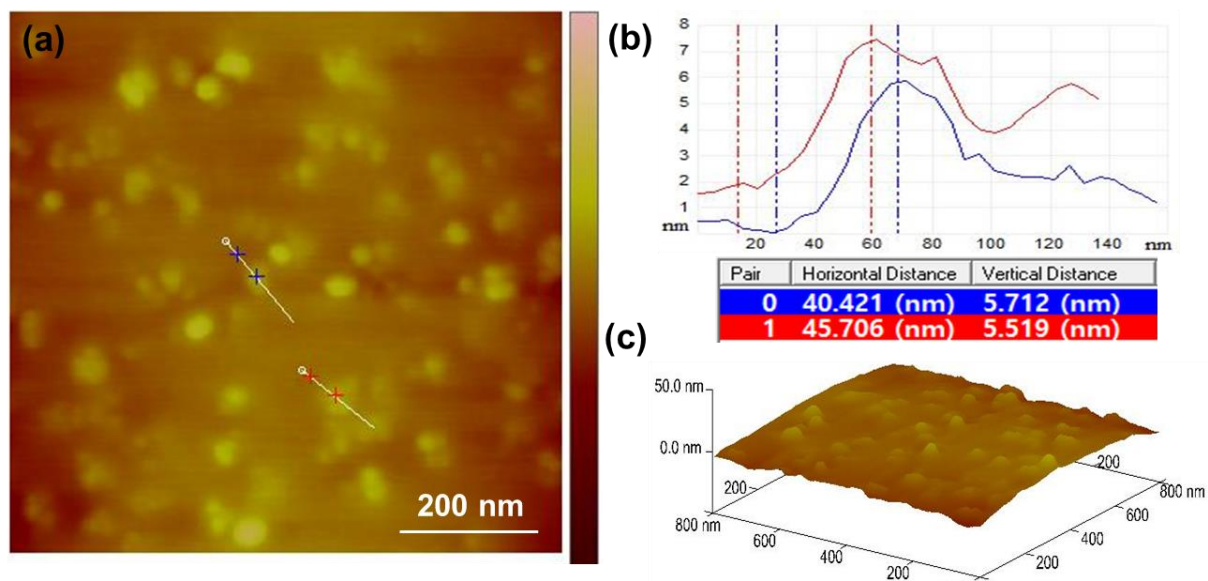


Figure S3 | Surface characteristics of flexible SERS sensors. (a) AFM image, (b) height profile and (c) 3D image of the GNS array embedded in the PDMS film.

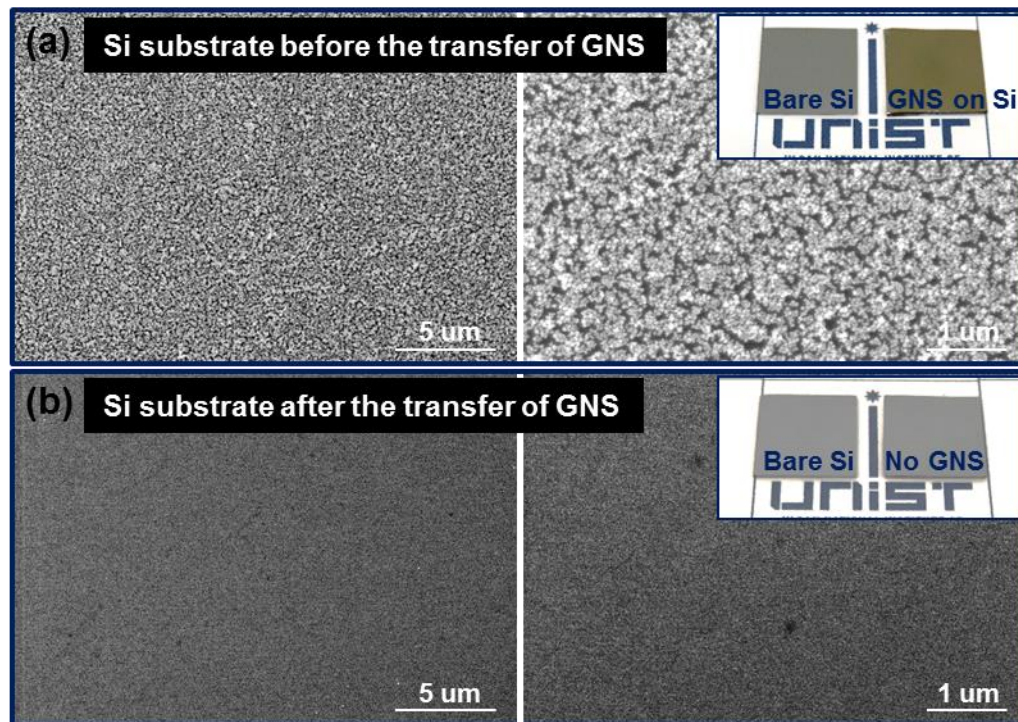


Figure S4 | SEM images of the Si substrates (a) before and (b) after the transfer of GNS array from Si substrate to PDMS. The insets are photo images of GNS array on the Si substrate before and after the transfer of the GNS array in comparison with the bare Si substrate.

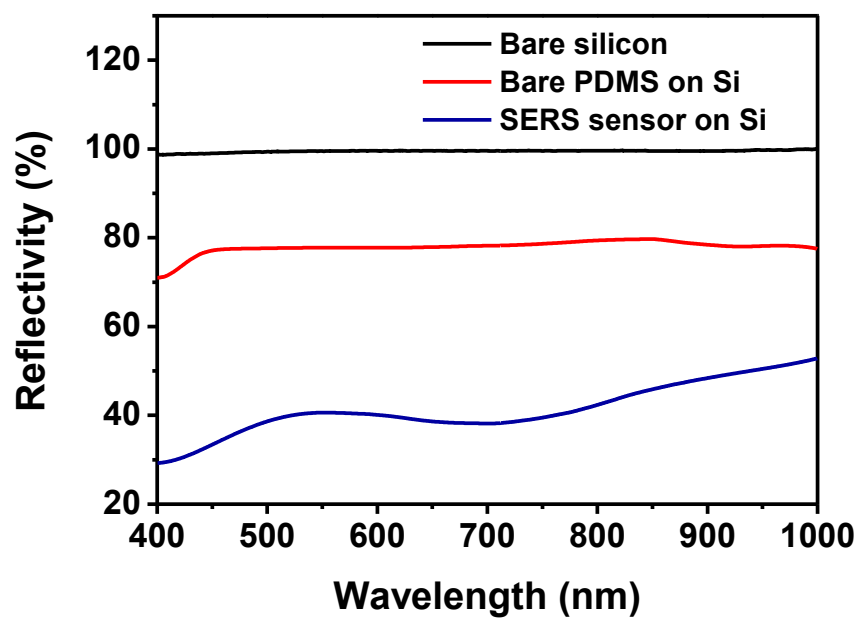


Figure S5 | Reflectivity spectra of bare silicon, bare PDMS on Si substrate and SERS sensor on Si substrate.

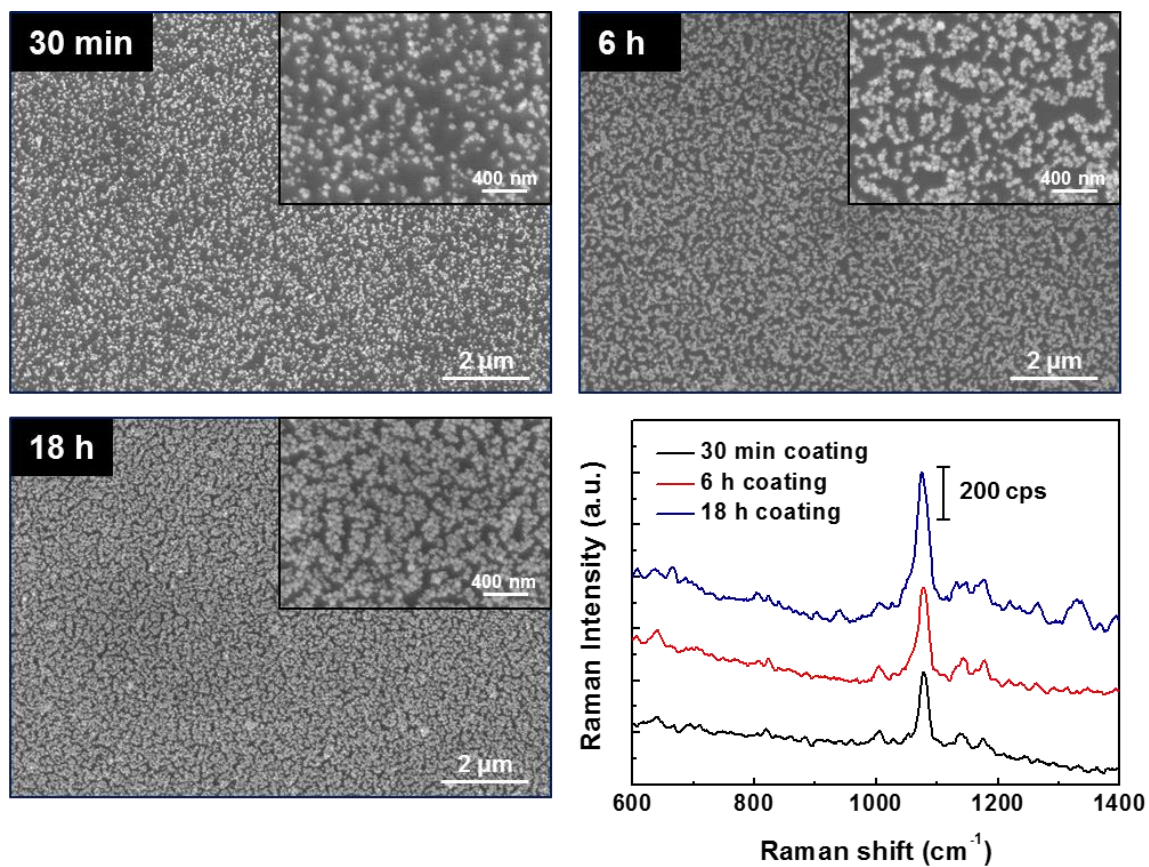


Figure S6 | GNS-density dependent SERS activity. SEM images of different-density GNS arrays for different coating times and the related SERS activity.

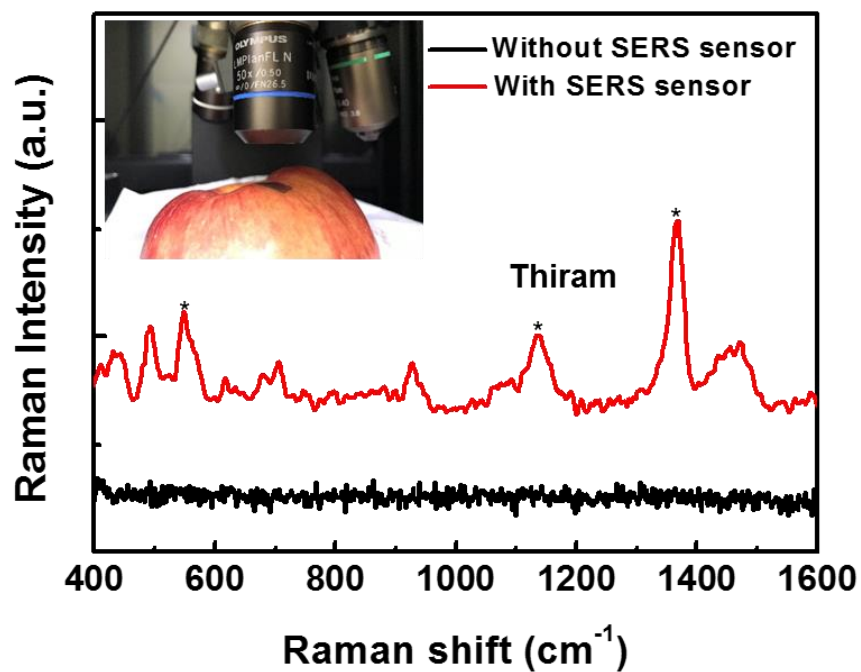


Figure S7 | SERS activity on the apple skin. Raman spectra of thiram (10^{-4} M) molecules adsorbed on the apple skin with and without covering of SERS sensors.

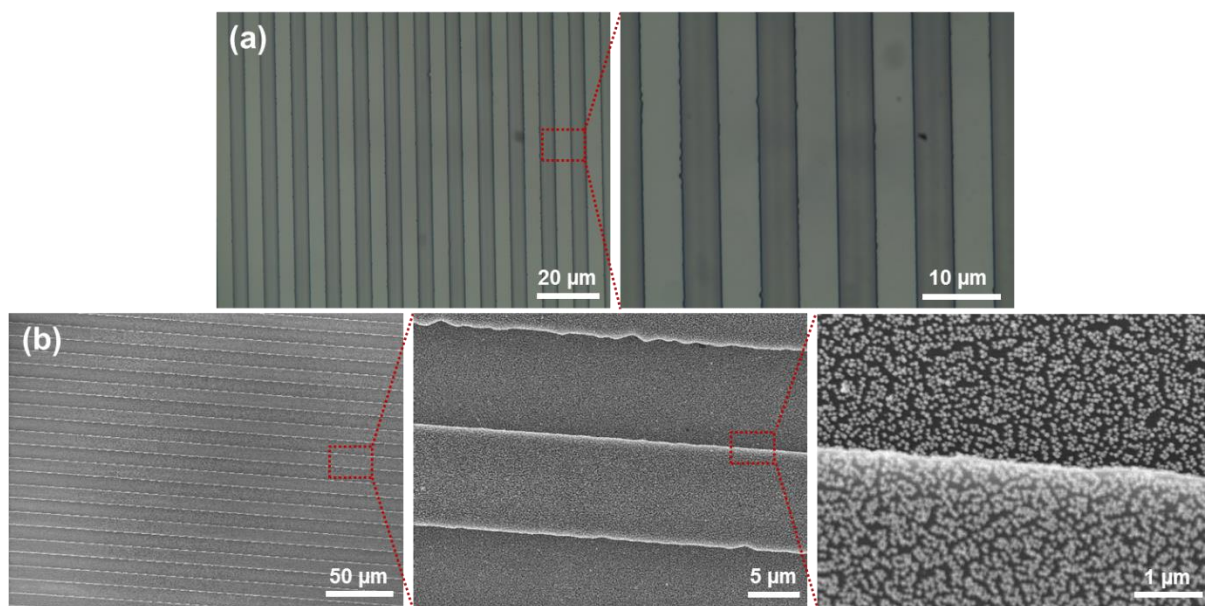


Figure S8 | (a) Optical microscope (OM) images of line-patterned Si substrate and (b) SEM images of GNS coated line-patterned Si substrate.

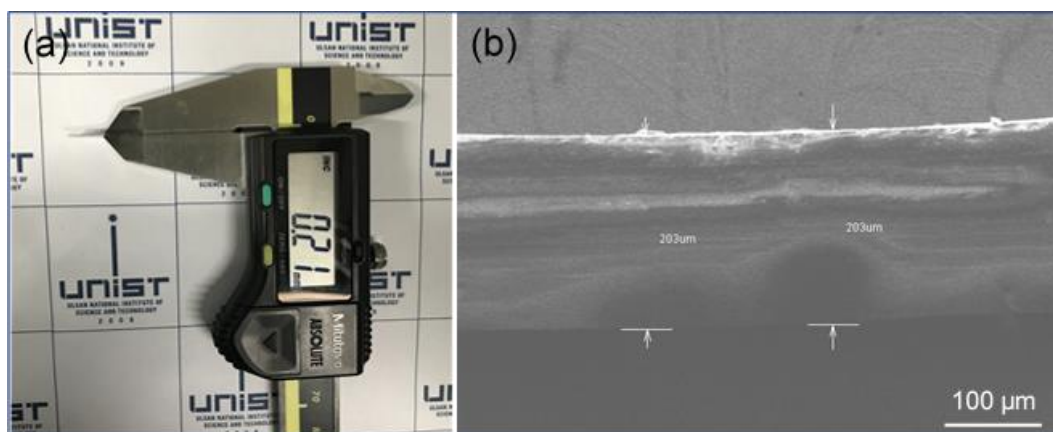


Figure S9 | Characteristics of SERS sensors. (a) Photo image and (b) SEM image of SERS sensor demonstrating the thickness of SERS film which is estimated to be $\sim 200\text{ }\mu\text{m}$.

Table S1 | Comparison table related to the GNS based SERS sensors.

SERS substrate	Analytes	Limit of detection (LOD)	Enhancement factor	Ref.
<i>Single GNS</i>	<i>Mercaptobenzoic acid</i>	$2 \times 10^{-3} \text{ M}$	10^7	1
<i>APTES-functionalized surface-assembly of GNS</i>	<i>Nile blue A</i>	$5 \times 10^{-11} \text{ M}$	5×10^6	2
	<i>Rhodamine 6G</i>	$1 \times 10^{-9} \text{ M}$	2×10^5	
<i>Flexible PDMS/gold nanostar *</i>	<i>Thiabendazole</i>	$2 \times 10^{-8} \text{ M}$	-	3
<i>Nano graphene oxide-wrapped GNS</i>	<i>Rhodamine B</i>	$1.5 \times 10^{-8} \text{ M}$	-	4
<i>GNS for detection of uranyl</i>	<i>Uranyl</i>	$1.2 \times 10^{-7} \text{ M}$	-	5
<i>GNS-Coated Polystyrene Beads</i>	<i>Mercaptobenzoic acid</i>	$1 \times 10^{-3} \text{ M}$	7.5×10^7	6
<i>GNS core-silver nanoparticle</i>	<i>Aflatoxin B1</i>	$3.2 \times 10^{-6} \text{ M}$	-	7
<i>GNS-ICG-BSA nanotags</i>	<i>Indocyanine green</i>	$1 \times 10^{-4} \text{ M}$	2.02×10^6	8
<i>Flexible AuNR/filter paper *</i>	<i>1,4-Benzenedithiol</i>	$1 \times 10^{-10} \text{ M}$	5×10^6	9
<i>Flexible AgNP/filter paper by brushing technique *</i>	<i>R6G</i>	$4.5 \times 10^{10} \text{ M}$	2.2×10^7	10
<i>Flexible free-standing silver nanoparticles-graphene *</i>	<i>R6G</i>	-	1.25×10^7	11
<i>Flexible AuNR/PVA electrospun mats *</i>	<i>3,3'-diethylthiatri-carbocyanine iodide</i>	10^{-4} M	-	12
<i>Flexible GNS/PDMS *</i>	<i>Benzenethiol</i>	$1 \times 10^{-8} \text{ M}$	1.9×10^8	<i>This work</i>
<i>* Flexible SERS sensor</i>				

References

- (1) Hrelescu, C.; Sau, T. K.; Rogach, A. L.; Jäckel, F.; Feldmann, J. Single gold nanostars enhance Raman scattering. *Appl. Phys. Lett.* **2009**, *94*, 153113.
- (2) Su, Q.; Ma, X.; Dong, J.; Jiang, C.; Qian, W. A reproducible SERS substrate based on electrostatically assisted APTES-functionalized surface-assembly of gold nanostars. *ACS Appl. Mater. Interfaces* **2011**, *3*, 1873-1879.
- (3) Shiohara, A.; Langer, J.; Polavarapu, L.; Liz-Marzan, L. M. Solution processed polydimethylsiloxane/gold nanostar flexible substrates for plasmonic sensing. *Nanoscale* **2014**, *6*, 9817-9823.
- (4) Jalani, G.; Cerruti, M. Nano graphene oxide-wrapped gold nanostars as ultrasensitive and stable SERS nanoprobe. *Nanoscale* **2015**, *7*, 9990-9997.
- (5) Lu, G.; Forbes, T. Z.; Haes, A. J. SERS detection of uranyl using functionalized gold nanostars promoted by nanoparticle shape and size. *Analyst* **2016**, *141*, 5137-5143.
- (6) Serrano-Montes, A. B.; Langer, J.; Henriksen-Lacey, M.; Jimenez de Aberasturi, D.; Solís, D. M.; Taboada, J. M.; Obelleiro, F.; Sentosun, K.; Bals, S.; Bekdemir, A.; Stellacci, F.; Liz-Marzan, L. M. Gold nanostar-coated polystyrene beads as multifunctional nanoprobe for SERS bioimaging. *J. Phys. Chem. C* **2016**, *120*, 20860-20868.
- (7) Li, A.; Tang, L.; Song, D.; Song, S.; Ma, W.; Xu, L.; Kuang, H.; Wu, X.; Liu, L.; Chen, X.; Xu, C. A SERS-active sensor based on heterogeneous gold nanostar core-silver nanoparticle satellite assemblies for ultrasensitive detection of aflatoxinB1. *Nanoscale* **2016**, *8*, 1873-1878.
- (8) Chen, J.; Sheng, Z.; Li, P.; Wu, M.; Zhang, N.; Yu, X. F.; Wang, Y.; Hu, D.; Zheng, H.; Wang, G. P. Indocyanine green-loaded gold nanostars for sensitive SERS imaging and subcellular monitoring of photothermal therapy. *Nanoscale* **2017**, *9*, 11888-11901.
- (9) Lee, C. H.; Tian, L.; Singamaneni, S. Paper-based SERS swab for rapid trace detection on real-world surfaces. *ACS Appl. Mater. Interfaces* **2010**, *2*, 3429-3435.
- (10) Zhang, W.; Li, B.; Chen, L.; Wang, Y.; Gao, D.; Ma, X.; Wu, A. Brushing, a simple way to fabricate SERS active paper substrates. *Anal. Methods* **2014**, *6*, 2066.
- (11) Zhou, Y.; Cheng, X.; Yang, J.; Zhao, N.; Ma, S.; Li, D.; Zhong, T. Fast and green synthesis of flexible free-standing silver nanoparticles-graphene substrates and their surface-enhanced Raman scattering activity. *RSC Adv.* **2013**, *3*, 23236.
- (12) Zhang, C. L.; Lv, K. P.; Cong, H. P.; Yu, S. H. Controlled Assemblies of Gold Nanorods in PVA Nanofiber Matrix as Flexible Free-Standing SERS Substrates by Electrospinning. *Small* **2012**, *8*, 648-653.